

Integrability to chaos transition through Krylov approach for state evolution

Gastón F. Scialchi,^{1,2,*} Augusto J. Roncaglia,^{1,2} and Diego A. Wisniacki^{1,2,†}

¹*Universidad de Buenos Aires, Facultad de Ciencias Exactas y Naturales, Departamento de Física. Buenos Aires, Argentina*

²*CONICET - Universidad de Buenos Aires, Instituto de Física de Buenos Aires (IFIBA). Buenos Aires, Argentina*

The complexity of quantum evolutions can be understood by examining their dispersion in a chosen basis. Recent research has stressed the fact that the Krylov basis is particularly adept at minimizing this dispersion [V. Balasubramanian et al, Physical Review D 106, 046007 (2022)]. This property assigns a central role to the Krylov basis in the investigation of quantum chaos. Here, we delve into the transition from integrability to chaos using the Krylov approach, employing an Ising spin chain and a banded random matrix model as our testing models. Our findings indicate that both the saturation of Krylov complexity and the dispersion of the Lanczos coefficients can exhibit a significant dependence on the initial condition. However, both quantities can gauge dynamical quantum chaos with a proper choice of the initial state.

I. INTRODUCTION

The field of quantum chaos has made significant advancements in unraveling the intricacies of quantum systems by characterizing their spectral properties through the utilization of random matrix models associated with various statistical ensembles [1, 2]. This statistical framework has also proven invaluable in portraying the attributes of quantum systems with many-body interactions, where a classical depiction is elusive [3]. Consequently, a measure of chaos in these systems typically revolves around their spectral patterns. In conjunction with this spectral perspective on quantum chaos, an additional venue of exploration delves into the analysis of their dynamics. This entails exploring measures like the Loschmidt echo and out-of-time-ordered correlators (OTOCs) which provide insight into the system's irreversibility when subjected to perturbations and the propagation behavior of operators as they evolve in time [4–7].

A novel addition to the dynamic approach is known as Krylov complexity (\mathcal{K} -complexity) [8]. This measure was developed for both Schrödinger evolution of states [9] and Heisenberg evolution of observables in an operator Hilbert space formed via a suitable inner product [10]. It is derived using the Lanczos algorithm that, given an initial condition, yields a series of values referred to as Lanczos coefficients and an orthonormal basis for the Krylov subspace that encompasses the system evolution. This algorithm transforms the original system into a one-dimensional tight-binding problem with disordered attributes, where the hopping amplitudes are determined by the Lanczos coefficients. The concept of \mathcal{K} -complexity is then established as the dispersion of the one-particle wavefunction across the Krylov space.

Under operator formalism, it has been hypothesized [8] that generic chaotic systems in the thermodynamic limit exhibit an exponential growth of \mathcal{K} -complexity, which sharply bounds the Lyapunov exponent as defined

through the growth of OTOCs. Further research has been done in finite systems [10–13], where it was conjectured and observed that chaotic systems exhibit a larger long-time saturation value of \mathcal{K} -complexity when compared to integrable ones, and that this can be understood as Anderson localization in the associated tight-binding problem due to the Lanczos sequences derived from integrable systems having more disorder. However, this seems not to be universal due to its strong dependency on the chosen initial operator [14].

The goal of this study is to explore the transition from integrability to chaos using the Krylov formalism applied to quantum states [9]. To achieve this goal, we examine the dynamics of \mathcal{K} -complexity saturation, Lanczos coefficient dispersion, and how these vary in relation to the level of chaos present within the system. We do this by performing a numerical study of the aforementioned quantities along with the parametric integrability-to-chaos transition present in both an Ising spin chain subject to an external magnetic field and a banded random model [15–18]. Our research shows that both the saturation of Krylov complexity and the dispersion of Lanczos coefficients are influenced by the initial conditions. However, they can effectively assess the onset of dynamical quantum chaos when the initial state is carefully selected. We also found that the dispersion of the Lanczos coefficients shows a more robust behaviour for the initial conditions considered in this work.

This work is organized as follows. In Sec. II we briefly go over the Lanczos algorithm, define the Krylov complexity, and review both the relation between its long-time saturation value and the dispersion of Lanczos coefficients with chaos. In Sec. III A we present our numerical results for an Ising spin chain with a longitudinal-transverse magnetic field using a variety of initial states and explore the best choice in order to extract universal features of the system's complexity. An analogous study for a random banded model is shown in Sec. III B, in order to test how these results behave in the integrability-to-chaos transition for a generic system modeled through its spectral statistics. To highlight the importance of the choice of the initial state in the Krylov approach, in App.

* E-mail address: gscialchi@df.uba.ar

† E-mail address: wisniacki@df.uba.ar

B we analytically study the dependence of the Krylov complexity saturation with the energy localization of the initial state. We conclude in Sec. IV with a summary of our results and some final remarks.

II. LANCZOS ALGORITHM AND KRYLOV COMPLEXITY SATURATION

As an initial state $|\psi_0\rangle$ evolves in time, it traverses a fraction of the system Hilbert space known as the Krylov subspace. When considering the evolution under a time-independent Hamiltonian H :

$$|\psi(t)\rangle = e^{-itH} |\psi_0\rangle = \sum_{n=0}^{\infty} \frac{(-it)^n}{n!} H^n |\psi_0\rangle. \quad (1)$$

From this expression it is possible to obtain a basis for this subspace. For systems with a finite Hilbert space dimension D , only a finite number (denoted as K) of the states $H^n |\psi_0\rangle$ can be linearly independent. Therefore, the Krylov subspace is the space spanned by the successive applications of the Hamiltonian to the initial state,

$$\mathcal{K} = \text{span}\{H^n |\psi_0\rangle\}_{n=0}^{K-1}. \quad (2)$$

An orthonormal basis for \mathcal{K} can be obtained employing the Lanczos algorithm [19, 20] which recursively applies the Gram-Schmidt procedure to Eq. (2). In this way, the Krylov basis elements $\{|K_n\rangle\}_{n=0}^{K-1}$ are defined through

$$|A_{n+1}\rangle = (H - a_n) |K_n\rangle - b_n |K_{n-1}\rangle, \quad |K_n\rangle = b_n^{-1} |A_n\rangle, \quad (3)$$

where a_n and b_n are the Lanczos coefficients:

$$a_n = \langle K_n | H | K_n \rangle, \quad b_n = \sqrt{\langle A_n | A_n \rangle}, \quad (4)$$

obtained in terms of the initial conditions $b_0 = 0$ and $|K_0\rangle = |\psi_0\rangle$. This algorithm also transforms the Hamiltonian into a tridiagonal form,

$$H |K_n\rangle = a_n |K_n\rangle + b_{n+1} |K_{n+1}\rangle + b_n |K_{n-1}\rangle, \quad (5)$$

where a_n and b_n represent the diagonal and off-diagonal elements of the Hamiltonian in the Krylov basis. The Lanczos algorithm, as delineated in Eq. (3), can exhibit numerical instability due to the accumulation of roundoff errors stemming from floating-point computations. Various alternative implementations have been proposed to mitigate this issue, as outlined in [19, 21]. Here, we adopt the full orthogonalization variant of the algorithm.

The time-evolved state [Eq. (1)] expanded within the Krylov basis is:

$$|\psi(t)\rangle = \sum_{n=0}^{K-1} \psi_n(t) |K_n\rangle, \quad (6)$$

Then, incorporating Eq. (5) into the Schrödinger equation, an expression governing the evolution of the coefficients $\psi_n(t)$ can be derived,

$$i\partial_t \psi_n(t) = a_n \psi_n(t) + b_n \psi_{n-1}(t) + b_{n+1} \psi_{n+1}(t). \quad (7)$$

This expression indicates that the evolution of $|\psi_0\rangle$ can be obtained in terms of that of a one-dimensional tight-binding problem. With this analogy, the hopping and site coefficients are dictated by the Lanczos sequences, and the initial condition of the tight-binding problem is completely localized at the leftmost site of the chain ($\psi_n(0) = \delta_{n0}$). Starting from $t = 0$, where only the element $|K_0\rangle$ of the Krylov basis is relevant, the wavefunction $\psi_n(t)$ progressively permeates further into the expanse of the Krylov space as time goes on. This expansion prompts the requirement for an increasing number of basis elements to faithfully capture the unfolding evolution. This realization naturally leads to the concept of evolution complexity referred to as Krylov complexity [8, 10], which is defined as the average spatial position of the wavefunction throughout the chain,

$$C_{\mathcal{K}}(t) = \sum_{n=0}^{K-1} n |\psi_n(t)|^2. \quad (8)$$

This value encapsulates the average dimension of the Krylov subspace representing the evolution from the initial state up to time t . We note that, with the exception of exact degeneracies in the Hamiltonian spectrum caused by symmetries, the Krylov subspace that encapsulates the evolution of the system for all times covers the entire Hilbert space in all the scenarios that we have studied. Furthermore, we have observed that the presence of such exact degeneracies can introduce numerical instability in the Lanczos algorithm, even when employing the full orthogonalization routine. This challenge can be circumvented by confining the Hamiltonian to a symmetry subspace. We further assume an absence of accidental degeneracies in the spectrum of the Hamiltonian. For this reason, we set $K = D$, understanding that the Krylov basis expands the full Hilbert space or a symmetry subspace of dimension D .

In this work we are mainly interested on the long-time saturation value of the \mathcal{K} -complexity which, by a procedure completely analogous to the one presented in Ref. [12], can be shown to follow

$$\overline{C_{\mathcal{K}}} \equiv \lim_{T \rightarrow \infty} \frac{1}{T} \int_0^T dt C_{\mathcal{K}}(t) = \sum_{n=0}^{D-1} n Q_{0n}, \quad (9)$$

where

$$Q_{0n} \equiv \sum_{i=1}^D |\langle e_i | \psi_0 \rangle|^2 |\langle K_n | e_i \rangle|^2 \quad (10)$$

and $H |e_i\rangle = e_i |e_i\rangle$. By expanding the eigenstates of the Hamiltonian in the Krylov basis $|e_i\rangle = \sum_{n=0}^{D-1} \varepsilon_n^i |K_n\rangle$ and using Eq. (5) we obtain a related tight-binding problem:

$$e_i \varepsilon_n^i = a_n \varepsilon_n^i + b_n \varepsilon_{n-1}^i + b_{n+1} \varepsilon_{n+1}^i, \quad (11)$$

where $|\varepsilon_n^i|^2 = |\langle K_n | e_i \rangle|^2$.

Under the operator formalism (where $a_n = 0 \forall n$) it was proposed in [12], and observed in certain systems in [13], that the saturation value [Eq. (9)] should be larger for chaotic systems than for integrable ones. It is argued heuristically that an abundance of quasidegeneracies in the spectrum of the system leads to an erratic behavior of the Lanczos coefficients b_n . As a consequence, the relation in Eq. (11) describes a tight-binding problem with off-diagonal disorder, which is subject to Anderson localization. As integrable systems are typically characterized by Poissonian level spacing statistics, they present a high degree of quasidegeneracies leading to a larger disorder. Conversely, the level repulsion present in chaotic systems implies less disorder, and a more delocalized wavefunction. The same argument may be extended to the state formalism with the addition of diagonal disorder. We then have, in the completely delocalized limit, $|\varepsilon_n^i|^2 = 1/D \forall i, n$ and from Eq. (9):

$$\overline{C_K} = \frac{1}{D} \sum_{n=0}^{D-1} n = \frac{D-1}{2}. \quad (12)$$

In this study, we also aim to investigate the relation between chaotic behavior and the dispersion of the Lanczos coefficients under state formalism. The localization length L_{loc} of the wavefunction has been proposed to be related to the amount of disorder in the off-diagonal sequence through [22]

$$L_{\text{loc}} \propto \sigma_{\log}^{-1}(b_n), \text{ where } \sigma_{\log}^2(b_n) = \text{Var} \left(\ln \left| \frac{b_{2n-1}}{b_{2n}} \right| \right). \quad (13)$$

This dispersion measure can suffer from large fluctuations when the Lanczos sequence is small, which may be the case for a_n since it typically fluctuates around zero for sufficiently large n (as Fig. 1.(a) shows). An intuitive alternative definition is to measure the dispersion of the sequences with respect to their local mean. Given a sequence s_n of length N , the dispersion about its moving average is

$$\sigma^2(s_n) \equiv \frac{1}{N} \sum_{n=n_0}^N (s_n - \bar{s}_n)^2, \text{ with } \bar{s}_n = \frac{1}{2w} \sum_{m=n-w}^{n+w} s_m, \quad (14)$$

where w is the half-width of the window used to compute the moving average and n_0 the value of the sequence index from which to start computing the dispersion. We show in Fig. 1 an example of the quantities just described applied to an instance of Lanczos sequences. For the data in the figure (and for the rest of the results in this work) we chose $w = 0.025N$, and a value of n_0 so as to avoid the initial ramp in the sequences. A comparison between both measures of dispersion can be seen in Fig. 2. For the sequence b_n , both definitions (13) and (14) agree [see Fig. 2.(b)], but it is not the case when applied to a_n [Fig. 2.(a)]. Moreover, the functional shape of $\sigma(a_n)$ is almost identical to that of $\sigma(b_n)$, except for

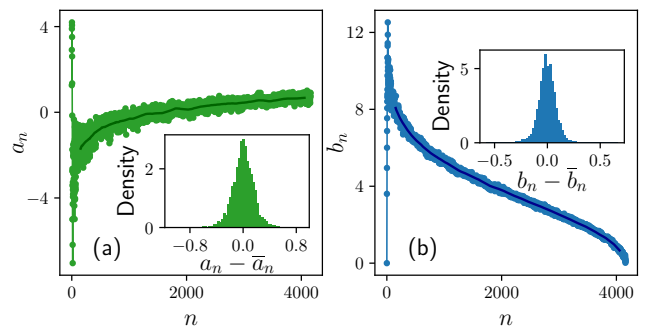


Figure 1. Example of the (a) diagonal and (b) off-diagonal Lanczos sequences and their moving averages (dark lines). The insets show the distribution of the fluctuations of the sequences about said moving averages. These sequences correspond to the Ising model discussed in Sec. III A with a value of the magnetic field component $h_z = 1.02$.

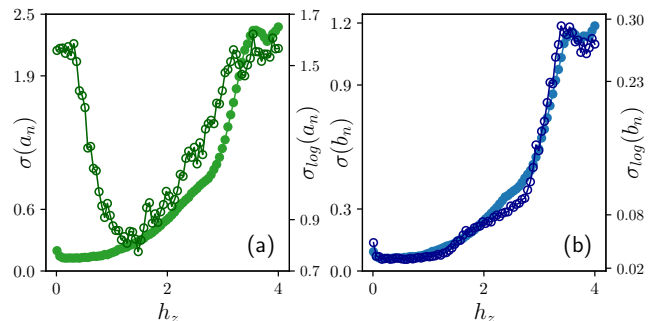


Figure 2. Comparison of Lanczos coefficient dispersion measures applied to the (a) diagonal and (b) off-diagonal sequences as a function of the magnetic field component h_z in the Ising model discussed in Sec. III A. The filled circles correspond to the dispersion definition in Eq. (14), while the dark empty circles to that of Eq. (13).

a rescaling factor. The data shown in Figs. 1 and 2 were obtained using the Ising model discussed in Sec. III A restricted to the positive parity subspace, and the initial state with all $N = 13$ spins in the 'up' configuration.

III. GAUGING QUANTUM COMPLEXITY THROUGH KRYLOV EVOLUTION OF STATES

Here we present numerical results for the quantities detailed in the previous section. Namely, the saturation of Krylov complexity [Eq. (9)] and the dispersion of the Lanczos coefficients [Eq. (14)]. We trace these quantities along the integrability to chaos transition of an Ising spin chain in Sec. III A and an statistical ensemble transition for a banded random matrix model in Sec. III B, comparing them with the spectral statistics of each system as a quantifier of quantum chaos. This is done for various initial states.

The spectral measure of chaos that we used is the mean

value of the ratio of consecutive energy level spacings $s_i = e_i - e_{i-1}$ [23],

$$\langle \tilde{r} \rangle = \frac{1}{D} \sum_{n=1}^D \tilde{r}_n, \quad \text{where} \quad \tilde{r}_n = \frac{\min(s_n, s_{n-1})}{\max(s_n, s_{n-1})}, \quad (15)$$

which takes the values $\langle \tilde{r} \rangle_P \approx 0.38629$ for Poissonian statistics and $\langle \tilde{r} \rangle_{WD} \approx 0.53590$ for the orthogonal Gaussian ensemble. We normalize this quantity as

$$\eta = \frac{\langle \tilde{r} \rangle - \langle \tilde{r} \rangle_P}{\langle \tilde{r} \rangle_{WD} - \langle \tilde{r} \rangle_P} \quad (16)$$

to obtain a measure of quantum chaos such that $\eta \approx 1$ for a chaotic system and $\eta \approx 0$ for an integrable system.

A. Integrability-to-chaos transition in a spin chain

We consider an Ising model with nearest-neighbor interactions in the z direction and a magnetic field on the $x - z$ plane given by the Hamiltonian

$$H = \sum_{i=1}^N (\sigma_x^{(i)} + h_z \sigma_z^{(i)}) - \sum_{i=1}^{N-1} \sigma_z^{(i)} \sigma_z^{(i+1)}, \quad (17)$$

where N is the number of spin-1/2 particles in the chain and $\sigma_k^{(i)}$ the Pauli operator at the i -th site in the direction k . This model exhibits an integrability-to-chaos transition as a function of the longitudinal component of the magnetic field h_z , such that the system is integrable for $h_z = 0$ and $h_z \gg 1$, and chaotic when $h_z \sim 1$.

We also consider open boundary conditions, which makes the system invariant under reflection with respect to the center of the chain. This implies that the Hamiltonian commutes with the parity operator, allowing it to be decomposed into disconnex even and odd parity subspaces of dimension $D^{\text{even/odd}} \simeq D/2$ such that the dimension of the full Hilbert space is $D = D^{\text{even}} + D^{\text{odd}}$. Here we restrict the dynamics to the even subspace. For $h_z = 0$ the system acquires an additional symmetry associated to the conservation of the magnetization, but we avoid this point in our calculations.

We have performed simulations for different values of h_z and considered different initial states. Figure 3 shows the saturation of \mathcal{K} -complexity [Eq. (9)] normalized by its approximate expected value for full delocalization in Krylov space [Eq. (12)]. In Figure 4 it is shown the inverse dispersion of the Lanczos coefficients [Eq. (14)] with a normalization that is detailed in Appendix A. Both quantities are compared with the chaoticity of the system as defined through Eq. (16). The curve for η was obtained by setting $N = 13$, while the complexity saturation and dispersion correspond to $N = 10$. The latter two remain invariant upon modifying the number of spins. The initial states we considered are: all spins in the 'up' state $|\psi_0^{\text{up}}\rangle$, a state uniformly spread over the energy eigenbasis with $h_z = 0$ $|\psi_0^{\text{unif}}\rangle$, random states $\{|\psi_0^{\text{rand}}\rangle\}$,

eigenstates of the integrable Hamiltonian with $h_z = 4$ $\{|\psi_0^{h_z=4}\rangle\}$, and eigenstates of the integrable Hamiltonian with $h_z = 0$ $\{|\psi_0^{h_z=0}\rangle\}$. In the last three cases we considered averages over the respective sets of states. For the random states the average was made over ten realizations of the initial state, and in the remaining two cases over forty states around the center of the energy spectrum of each respective integrable Hamiltonian. The results remain largely invariant as we increment the number of states in these averages.

As can be seen in Fig. 3, the saturation value of Krylov complexity exhibits a high dependence on the initial state. The curves corresponding to the states $|\psi_0^{\text{up}}\rangle$

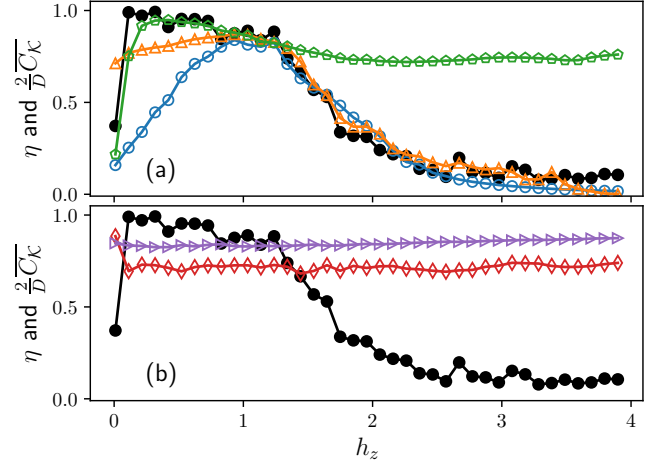


Figure 3. Chaotic measure η (black filled circles) and saturation of the \mathcal{K} -complexity as a function of the chaos parameter h_z through the chaos-to-integrability transition in the Ising spin chain for a variety of initial states. The complexity curves correspond to (a) an initial state in the all spins 'up' configuration (blue circles), an average over initial states from the eigenbasis of the integrable Hamiltonian with $h_z = 4$ (orange triangles), and an average over initial states from the eigenbasis of the integrable Hamiltonian with $h_z = 0$ (green pentagons), (b) average over random initial states (red diamonds) and an initial state uniformly distributed over the eigenbasis of the integrable Hamiltonian with $h_z = 0$ (purple triangles).

and the average over $\{|\psi_0^{h_z=4}\rangle\}$ [Fig. 3.(a)] display a remarkable correlation with the chaoticity quantifier η , although the former exhibits a decrease in complexity as h_z goes to zero even in regions where the system is still highly chaotic. For the average over the set $\{|\psi_0^{h_z=0}\rangle\}$ [Fig. 3.(a)], the saturation value of the Krylov complexity is high except in the region $h_z \approx 0$. On the other hand, when examining the uniformly distributed state and the average over random states [Fig. 3.(b)], there is no evident relationship between chaoticity and Krylov complexity saturation. In Appendix B, we analytically discuss the Krylov complexity saturation for uniformly distributed and energy-localized initial states.

The dependency of the saturation of \mathcal{K} -complexity on

the initial state contrasts with the behavior of the dispersion of the Lanczos coefficients, which varies less with the initial conditions studied in this work, as Fig. 4 shows. This observation applies for both the diagonal a_n and off-diagonal sequence b_n , and it is interesting to note that both also share a similar functional relation with respect to h_z , which holds true for all cases we consider in this

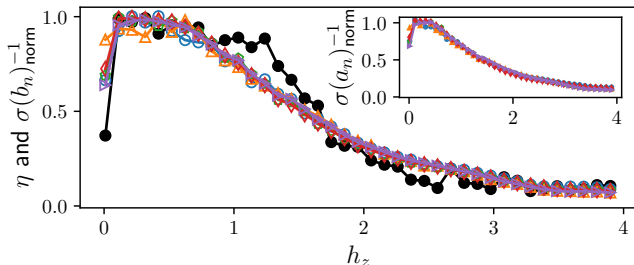


Figure 4. Chaotic measure η (black filled circles) and normalized inverse of the dispersion of Lanczos coefficients as a function of the chaos parameter h_z through the chaos-to-integrability transition in the Ising spin chain for a variety of initial states. The main plot shows the dispersion of the off-diagonal sequence b_n , while the inset that of the diagonal a_n (which has almost identical curves). Symbols of each curve are the same as in Fig. 3.

study. More importantly, we observe that the inverse of the dispersions of both diagonal a_n and off-diagonal b_n elements exhibit a striking resemblance to the spectral chaos measure η . In essence, they provide a more robust and accurate description of the chaos-integrability transition, surpassing the Krylov complexity, which is much more sensitive to the initial state.

Notice that the relation between the dispersion of the Lanczos coefficients and η that we have shown in this work is different from the one that was found in Ref. [14] under the Heisenberg picture. There, the chaotic transition as measured by η could be traced with $-\sigma$, while our current findings under the Schrödinger picture indicate that an accurate description can be achieved through the inverse of the dispersion $1/\sigma$. It would be interesting to explore the connection between the Krylov formalism within the Heisenberg picture and its counterpart within the Schrödinger picture.

For $h_z = 0$ the system gains an additional symmetry, and as such we have avoided this particular point. Nevertheless, its effects are still reflected on the spectral statistics in a small h_z region around the symmetry point. It is interesting to note that this feature also seems to have an impact on the saturation of \mathcal{K} -complexity [Fig. 3.(a)], and on the dispersion of the Lanczos coefficients [Fig. 4].

While it is not shown in this work, we have also observed that when the initial state is an eigenstate of the operator $\sum_{i=1}^{N-1} \sigma_k^{(i)} \sigma_k^{(i+1)}$ with $k = x, y$, both the \mathcal{K} -complexity saturation and the dispersion of Lanczos coefficients exhibit similarities to those observed in Figs. 3.(b) and 4, corresponding to $|\psi_0^{\text{unif}}\rangle$ and $\{|\psi_0^{\text{rand}}\rangle\}$ respec-

tively. This suggests that it is not required to select a fully delocalized or random state in order for the complexity saturation to fail in detecting the chaotic transition.

B. Integrability-to-chaos transition in a banded random model

To investigate the behavior of these quantities in generic systems, we consider a random matrix model. In particular, we study Hamiltonians obtained from banded random matrices of the form

$$H_{\text{RMT}} = \frac{H_0 + kV}{\sqrt{1 + k^2}}, \quad (18)$$

where H_0 is a diagonal matrix with elements drawn from a normal distribution with zero mean and unity variance, and V a real banded random matrix of bandwidth b [18]. Hence, this model exhibits a transition from Poissonian level statistics at $k = 0$ to GOE when k reaches a sufficiently large value. This is associated to the transition from a system with integrable dynamics to one that exhibits chaotic behavior. The dependence of H_{RMT} with k ensures that its spectrum remains bounded [24, 25].

The results for this model are shown in Figs. 5 and 6, and were obtained for a Hilbert space dimension of $D = 1024$ with a bandwidth $b = 0.2D$. Similarly to the previous approach, we have chosen the following initial states: an eigenstate of the Hamiltonian with $k = 0$ in the border of its spectrum $|\psi_0^{\text{b}}\rangle$, the uniformly spread state in the eigenbasis of the Hamiltonian with $k = 0$ $|\psi_0^{\text{unif}}\rangle$, random states $\{|\psi_0^{\text{rand}}\rangle\}$ and eigenstates of the Hamiltonian with $k = 0$ $\{|\psi_0^{k=0}\rangle\}$. For the first two, we considered an average over ten realizations of the random Hamiltonian. For the last two cases only one realization of the Hamiltonian was considered, while the averages were taken over ten random states, and twenty states around the center of the spectrum, respectively.

In Fig. 5, we can observe a relation of the \mathcal{K} -complexity with the initial state that is similar to what was found for the Ising model. While some states exhibit a discernible transition, others do not show any clear correlation. Namely, the \mathcal{K} -complexity corresponding to the states $|\psi_0^{\text{b}}\rangle$ and $\{|\psi_0^{k=0}\rangle\}$ is able to detect the transition [Fig 5.(a)]. On the other hand, for both the uniformly distributed state $|\psi_0^{\text{unif}}\rangle$ and the average over random states $\{|\psi_0^{\text{rand}}\rangle\}$ we observe a relatively high value of \mathcal{K} -complexity that is mostly insensitive to the transition [Fig 5.(b)].

The inverse of the dispersion of the Lanczos sequences shown in Fig. 6 can also be divided into two groups: one shows a strong resemblance to the spectral quantum measure η in describing the integrable-chaotic transition [Fig. 6.(a)], while the other [Fig. 6.(b)] does not exhibit such a straightforward correlation. In fact, as discussed in Appendix A, when the normalization is omitted, the last group exhibits higher values which may appear to

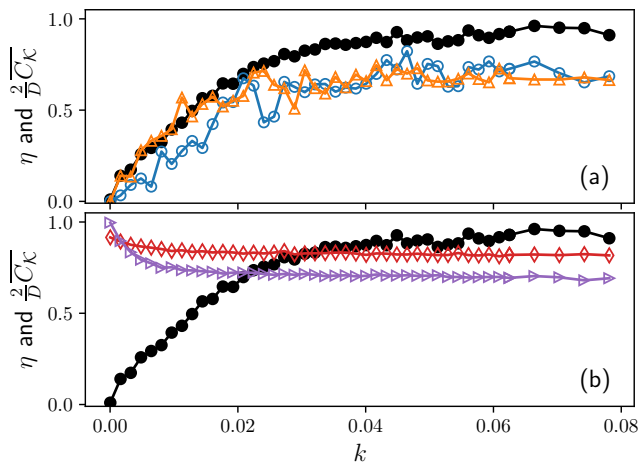


Figure 5. Chaotic measure η (black filled circles) and saturation of the \mathcal{K} -complexity as a function of the chaos parameter k through the Poisson-to-GOE ensemble transition for the banded random matrix model for a variety of initial states. The curves for the Krylov complexity correspond to (a) an initial state that is an eigenstate of H_{RMT} with $k = 0$ in the border of its spectrum (blue circles), an average over initial states from the eigenbasis of H_{RMT} with $k = 0$ (orange triangles), (b) an average over random initial states (red diamonds) and an initial state uniformly distributed over the eigenbasis of H_{RMT} with $k = 0$ (purple triangles).

imply a chaotic behavior for all values of k . It remains unclear whether this specific behavior can be observed in generic systems or if it originates solely from the random nature of this model.

IV. FINAL REMARKS

In this work we have extended previous analyses [13, 14] about the relationship between Lanczos coefficient dispersion, Krylov complexity saturation and chaos to the Schrödinger evolution of states. In order to accomplish this, we have taken into account an alternative interpretation of the Lanczos coefficient dispersion. This enables us to expand our analysis and examine situations where diagonal disorder is present within the state formalism. We have also investigated scenarios in which the saturation value of Krylov complexity is affected by the initial state. We found that when the initial states are widely spread in the energy eigenbasis of an integrable region, there may be an artificially high saturation value. On the contrary, if they are sufficiently localized, it tends to be suppressed. Both scenarios, upon initial examination, have the potential to mask the intrinsic chaotic or integrable nature of the Hamiltonian. On the other hand, the dispersion of the Lanczos coefficients seems to be less affected by the initial state.

The situation becomes more interesting when considering initial states that correspond to eigenstates within

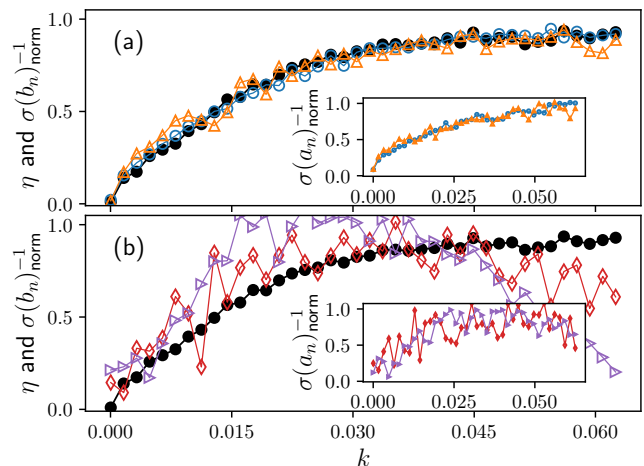


Figure 6. Chaotic measure η (black filled circles) and normalized inverse of the dispersion of Lanczos coefficients as a function of the chaos parameter k through the Poisson-to-GOE ensemble transition for the banded random matrix model for a variety of initial states. The main plots show the dispersion of the off-diagonal sequence b_n , while the insets that of the diagonal a_n (which has almost identical curves). Symbols for each curve and panel distribution are the same as in Fig. 5.

the integrable region. In this case, our numerical studies show that the Krylov complexity is closely aligned with the system's chaoticity measured by η . Notably, in such cases, the normalized complexity follows almost exactly the spectral measure of chaoticity for a significant range of parameters adjacent to those linked with the initial condition [see Figs. 3.(a) and 5.(a)]. It should be noted that local purity can also serve as a dynamic indicator of quantum chaotic behavior, although its computation is not as straightforward [17]. Therefore, in our case the choice of these initial states can be seen as analogous to determining the part of the Hamiltonian with lower complexity. In other words, the complexity is evaluated in relation to a particular Hamiltonian. In the case of the Ising model, where the region of chaotic behavior lies between two regions of integrability, even an integrable Hamiltonian can exhibit increased complexity for these initial conditions. In this scenario, the complexity arises not from the chaotic nature of the Hamiltonian itself. Consequently, it would be interesting to investigate if there exists an initial condition that can accurately track and reflect the spectral measure associated with chaos across all the range of parameters. We believe that this would provide additional insights into the intricate connection between Krylov complexity and quantum chaos.

V. ACKNOWLEDGMENTS

This work has been partially supported by CONICET (Grant No. PIP 11220200100568CO), UBACyT (Grant No. 20020170100234BA) and ANPCyT (PICT-2020-

SERIEA-01082, PICT-2021-I-A-00654, PICT-2021-I-A-01288).

Appendix A: Normalization for the Lanczos coefficient dispersion

In this work we compare the quantities of interest with the chaotic measure η , which is normalized to fit between the values 0 and 1 for an integrable and chaotic system, respectively. In order to make these comparisons more straightforward we would like to also map the saturation value of the Krylov complexity and the dispersion of Lanczos coefficients to the range $[0, 1]$, in a way that they share the same systematic as η does with chaos. The saturation value of the Krylov complexity possesses a natural normalization, since we expect $\overline{C_K} \sim 0$ for an integrable system and $\overline{C_K} \sim \frac{D}{2}$ for a chaotic one, but it is not the case for the dispersion of the Lanczos coefficients.

We address this issue by employing the normalization explained in Ref. [14]. Given a sequence of values X , we map it to that of η by rescaling as $X' = X \frac{\max \eta - \min \eta}{\max X - \min X}$ and applying a displacement such that fluctuations in the estimation of $\min X$ don't propagate to the whole rescaled sequence. This displacement minimizes the Euclidean distance of X' to η : $d_{\min}(X', \eta) = \min_{\alpha} \|(X' - \alpha) - \eta\|$. Thus, the normalized sequence is defined as

$$X_{\text{norm}} = X' - d_{\min}(X', \eta). \quad (\text{A1})$$

In the main text [Figs. 4 and 6] we show the inverse of the dispersion of the Lanczos sequences under this normalization, i.e., $X = 1/\sigma(a_n)$ and $X = 1/\sigma(b_n)$. Here, we show in Figs. 7 and 8 the same curves without normalizing, and the conclusions of this work remain the same. However, since the normalization is applied separately to each curve, this normalized dispersion measure is relative. As a result, while it could already be seen for the RMT model in Fig. 6.(b) that the curves corresponding to the uniform and random states do not accurately follow chaoticity, here it is made explicit that these curves show a high value of inverse dispersion irrespective of the chaos parameter k .

Appendix B: Krylov complexity saturation dependence on initial state energy localization

In the main part of the paper we have shown numerically that both the evolution of the Krylov complexity and its saturation value are tied to the initial state of the system. To reinforce the idea that choosing an appropriate initial state is essential to measure the complexity of a system through the Krylov approach, we show in this appendix two limiting cases of initial states such that the saturation of Krylov complexity is almost independent on the spectrum of the Hamiltonian, and are therefore not reliable for probing the chaoticity of the system.

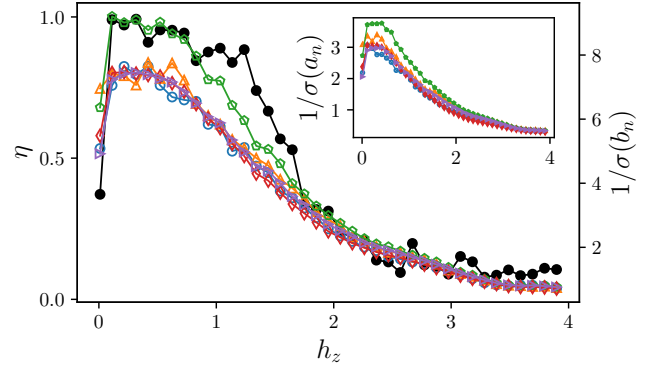


Figure 7. Chaotic measure η (black filled circles) and (not normalized) inverse of the dispersion of Lanczos coefficients as a function of the chaos parameter h_z through the chaos-to-integrability transition in the Ising spin chain for a variety of initial states. The main plot shows the dispersion of the off-diagonal sequence b_n , while the inset that of the diagonal a_n (which has almost identical curves, save for a rescaling factor). The indicators for each curve are the same as in Fig. 3.

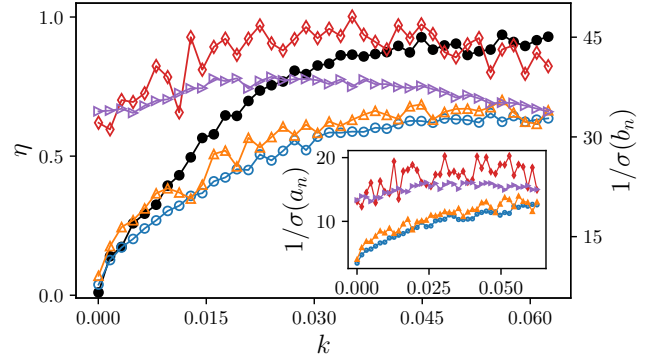


Figure 8. Chaotic measure η (black filled circles) and (not normalized) inverse of the dispersion of Lanczos coefficients as a function of the chaos parameter k through the Poisson-to-GOE ensemble transition for the banded random matrix model for a variety of initial states. The main plot shows the dispersion of the off-diagonal sequence b_n , while the inset that of the diagonal a_n (which has almost identical curves, save for a rescaling factor). The indicators for each curve are the same as in Fig. 5.

The first one is an initial state completely delocalized in the energy eigenbasis, such that $|\langle e_i | \psi_0 \rangle|^2 = 1/D \forall i$, and so Eq. (9) yields

$$\overline{C_K} = \frac{D-1}{2}. \quad (\text{B1})$$

This result is analogous to (12), but in that case the delocalization is of the Krylov basis elements over the energy eigenbasis. Under operator formalism, it was already shown in [13] that for an operator proportional to a matrix of ones in the energy eigenbasis, the saturation of Krylov complexity is $\overline{C_K} \sim \frac{K}{2} \sim \frac{D^2}{2}$ independently of the

spectrum of the Hamiltonian. Here D^2 is the dimension of the operator Hilbert space.

The opposite (and trivial) scenario is an initial state completely localized in the energy eigenbasis (an eigenstate of the Hamiltonian), and as such a stationary state. The Lanczos algorithm (3) will halt immediately in this case, yielding $b_n = 0$ and $|K_n| = 0 \forall n \geq 1$, and so $C_K(t) = 0$. In this sense, it may not be obvious whether the output of Lanczos algorithm is a "continuous function" of the initial state, meaning whether or not any initial state sufficiently localized in the energy eigenbasis will exhibit a low (suppressed) \mathcal{K} -complexity.

To explore this, consider such a state of the form

$$|\psi_0\rangle = \frac{1}{\sqrt{1+\delta^2}}(|e_j\rangle + \delta|\tilde{e}_j\rangle), \quad (\text{B2})$$

where $H|e_j\rangle = e_j|e_j\rangle$ and $\langle e_j|\tilde{e}_j\rangle = 0$, and the parameter δ controls the degree of localization. Under the assumption that either (i) the state $|\tilde{e}_j\rangle$ is delocalized in the remaining orthogonal part of the energy eigenbasis or that (ii) the Hamiltonian H can be modeled by a random matrix, by plugging the initial state (B2) into (10) we get, up to second order in δ ,

$$Q_{0n} = \left(f_n + \frac{1}{D-1}\right)\delta^2 + \mathcal{O}(\delta^4). \quad (\text{B3})$$

This is so because, under the above assumption, we may write $|\langle e_i|\tilde{e}_j\rangle|^2 \sim 1/(D-1)$ for a generic choice of $|\tilde{e}_j\rangle$, where the denominator is $D-1$ as opposed to D since $\langle e_j|\tilde{e}_j\rangle = 0$, and so $\sum_{i \neq j}^D |\langle K_n|e_i\rangle|^2 = 1 - |\langle K_n|e_j\rangle|^2$. Additionally, to obtain (B3), we show in Appendix C that the projection of the eigenvector $|e_j\rangle$ onto the Krylov basis follows $|\langle K_n|e_j\rangle|^2 = f_n\delta^2 + \mathcal{O}(\delta^4)$ for all $n \geq 1$.

Following (9), both terms in (B3) must be multiplied by n and summed, which is straightforward for the second one: $\sum_{n=0}^{D-1} \frac{n}{D-1} = \frac{D}{2}$. On the other hand, the sum of the first term is $\sum_{n=0}^{D-1} n f_n$, and can be bounded by taking advantage of the fact that

$$\sum_{n=1}^{D-1} f_n = \frac{1}{1+\delta^2}, \quad \text{with } f_n \geq 0, \quad (\text{B4})$$

which follows from normalization $\sum_{n=0}^{D-1} |\langle K_n|e_j\rangle|^2 = 1$, and noting that $|\langle K_0|e_j\rangle|^2 = |\langle \psi_0|e_j\rangle|^2 = 1/(1+\delta^2)$. From (B4), we obtain the bound

$$\sum_{n=0}^{D-1} n f_n \leq \frac{D-1}{1+\delta^2} = D-1 + \mathcal{O}(\delta^2). \quad (\text{B5})$$

Finally, we arrive to

$$\overline{C_K} \leq \left(\frac{3}{2}D-1\right)\delta^2 + \mathcal{O}(\delta^4). \quad (\text{B6})$$

In Figs 9 and 10 we show a comparison between the bound and the saturation of Krylov complexity for the

models considered in Secs. III A (with $N = 9$ and in the positive parity subspace) and III B (with $D = 256$), and initial states of the form (B2). This was done for different choices of j in $|e_j\rangle$ and $|\tilde{e}_j\rangle$, for the latter both delocalized and localized (such that the assumptions above don't necessarily apply), and in the integrable and chaotic regimes. In all cases the bound holds, up to rather large values of δ . The complexity curves get closer to the bound when both $|e_j\rangle$ and $|\tilde{e}_j\rangle$ are chosen near the center of the energy spectrum. The lowest saturation values are obtained when these are far apart from the center.

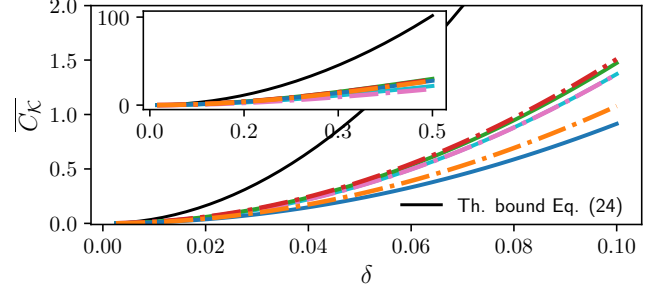


Figure 9. \mathcal{K} -complexity saturation for the Ising model studied in Sec. III A. The inset shows the same data as the main plot, but up to larger values of δ . The curves were obtained for $j = 10$, and $|\tilde{e}_j\rangle$ a Gaussian profile centered at $j = 61$ with standard deviation $\sigma = 10$ (blue and orange), $j = 60$ and $|\tilde{e}_j\rangle$ a Gaussian profile centered at $j = 61$ with standard deviation $\sigma = 10$ (green and red), and $j = 10$ and $|\tilde{e}_j\rangle$ uniformly distributed across the remaining orthogonal elements of the energy eigenbasis (cyan and pink), where the values for the index j assume an eigenbasis ordered according to increasing eigenvalues $e_j < e_{j+1}$. The solid lines correspond to $h_z = 4$, while the dash-dotted ones to $h_z = 0.5$.

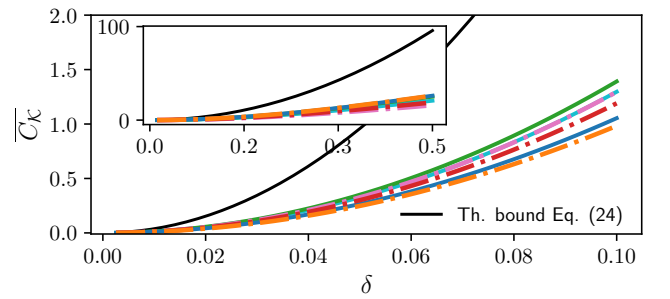


Figure 10. \mathcal{K} -complexity saturation for the random model studied in Sec. III B. The inset shows the same data as the main plot, but up to larger values of δ . The curves were obtained for initial states of the same form to those considered for Fig. 9, but here the solid lines correspond to $k = 0.000625$ and the dash-dotted ones to $k = 0.125$.

These results highlight the fact that in order to examine the overall chaoticity of the system through the use of the \mathcal{K} -complexity, the appropriate choice of initial state

may not be so obvious. For instance, an arbitrary initial state will be delocalized in the energy eigenbasis, leading to an "artificially" high complexity saturation. On the contrary, simpler states written in terms of the energy eigenbasis elements have their complexity saturation suppressed, obscuring the chaotic nature of the underlying Hamiltonian. This characteristic behavior with the initial state has also been observed in other metrics of quantum complexity, including the Loschmidt echo [4, 26, 27] and out-of-time-ordered correlators [28].

Appendix C: Dependence of the Krylov basis on the degree of localization

In this appendix we show that for an initial state of the form of Eq. (B2), the projection of the Krylov basis elements onto the eigenstate $|e_j\rangle$ follow $|\langle K_n | e_j \rangle|^2 = f_n \delta^2 + \mathcal{O}(\delta^4)$ with $f_n \geq 0$ for all $n \geq 1$, which is a necessary step in order to obtain the bound of Eq. (B6). We do this by explicitly carrying out the Lanczos algorithm (3) to the considered initial state up to $n = 3$, and then proceeding by induction.

Applying the Lanczos algorithm [Eq. (3)] to the initial

state Eq. (B2) up to $n = 3$ we obtain, for both $n = 2, 3$,

$$\begin{aligned} a_n &= a_n^{(0)} + a_n^{(2)} \delta^2 + \mathcal{O}(\delta^4), \\ b_n &= b_n^{(0)} + b_n^{(2)} \delta^2 + \mathcal{O}(\delta^4), \\ c_n &= c_n^{(0)} + c_n^{(2)} \delta^2 + \mathcal{O}(\delta^4) \end{aligned} \quad (C1)$$

and

$$\begin{aligned} |K_n\rangle &= (p_n^{(1)} \delta + p_n^{(3)} \delta^3) |e_j\rangle + \\ &\quad (q_n^{(0)} \delta + q_n^{(2)} \delta^2) |\tilde{e}_j\rangle + \mathcal{O}(\delta^4), \end{aligned} \quad (C2)$$

where $c_n \equiv \langle K_n | H^2 | K_n \rangle$, and both $p_n^{(m)}$ and $q_n^{(m)}$ are functions of the Hamiltonian H . For $n = 1$ these relations hold, except for $b_1 = b_1^{(1)} \delta + b_1^{(3)} \delta^3 + \mathcal{O}(\delta^5)$. For the purposes of this derivation, we are not concerned about the particular values the expansion coefficients $p_n^{(m)}$ and $q_n^{(m)}$ may take.

Now we proceed by induction. Suppose that for some n the relations in Eqs. (C1) and (C2) hold for both n and $n - 1$. By applying the Lanczos algorithm once again for the next iteration step, it is straightforward to check that these relations also hold for $n + 1$. Thus, since they hold for $n = 2$ and 3 , they do also for $n = 4$, and so, hold for all $n \geq 2$.

In particular, we have $|K_n\rangle = (p_n^{(1)} \delta + p_n^{(3)} \delta^3) |e_j\rangle + (q_n^{(0)} \delta + q_n^{(2)} \delta^2) |\tilde{e}_j\rangle + \mathcal{O}(\delta^4) \forall n \geq 1$, and so

$$|\langle K_n | e_j \rangle|^2 = p_n^{(1)2} \delta^2 + \mathcal{O}(\delta^4) \quad \forall n \geq 1, \quad (C3)$$

where we may identify $f_n = p_n^{(1)2} \geq 0$.

-
- [1] M. L. Mehta, *Random matrices* (Elsevier, 2004).
 - [2] S. Wimberger, *Nonlinear dynamics and quantum chaos*, Vol. 10 (Springer, 2014).
 - [3] K. Richter, J. D. Urbina, and S. Tomsovic, Semiclassical roots of universality in many-body quantum chaos, *Journal of Physics A: Mathematical and Theoretical* **55**, 453001 (2022).
 - [4] T. Prosen, T. H. Seligman, and M. Žnidarič, Dynamics of loschmidt echoes and fidelity decay, *Physics Reports* **435**, 33 (2006).
 - [5] A. Goussev, R. A. Jalabert, H. M. Pastawski, and D. A. Wisniacki, Loschmidt echo, *Scholarpedia* **7**, 11687 (2012).
 - [6] B. Swingle, Unscrambling the physics of out-of-time-order correlators, *Nature Physics* **14**, 988 (2018).
 - [7] T. Notenson, I. García-Mata, A. J. Roncaglia, and D. A. Wisniacki, Classical approach to equilibrium of out-of-time ordered correlators in mixed systems, *Physical Review E* **107**, 064207 (2023).
 - [8] D. E. Parker, X. Cao, A. Avdoshkin, T. Scaffidi, and E. Altman, A universal operator growth hypothesis, *Phys.Rev. X* **9**, 10.1103/physrevx.9.041017 (2019).
 - [9] V. Balasubramanian, P. Caputa, J. M. Magan, and Q. Wu, Quantum chaos and the complexity of spread of states, *Physical Review D* **106**, 10.1103/physrevd.106.046007 (2022).
 - [10] E. Rabinovici, A. Sánchez-Garrido, R. Shir, and J. Sonner, Operator complexity: a journey to the edge of krylov space, *J. High Energy Phys.* **2021** (6).
 - [11] J. Barbón, E. Rabinovici, R. Shir, and R. Sinha, On the evolution of operator complexity beyond scrambling, *Journal of High Energy Physics* **2019**, 1 (2019).
 - [12] E. Rabinovici, A. Sánchez-Garrido, R. Shir, and J. Sonner, Krylov localization and suppression of complexity, *Journal of High Energy Physics* **2022**, 10.1007/jhep03(2022)211 (2022).
 - [13] E. Rabinovici, A. Sánchez-Garrido, R. Shir, and J. Sonner, Krylov complexity from integrability to chaos, *Journal of High Energy Physics* **2022**, 10.1007/jhep07(2022)151 (2022).
 - [14] B. L. Español and D. A. Wisniacki, Assessing the saturation of krylov complexity as a measure of chaos, *Phys. Rev. E* **107**, 024217 (2023).
 - [15] M. C. Bañuls, J. I. Cirac, and M. B. Hastings, Strong and weak thermalization of infinite nonintegrable quantum systems, *Physical review letters* **106**, 050405 (2011).
 - [16] J. Li, R. Fan, H. Wang, B. Ye, B. Zeng, H. Zhai, X. Peng, and J. Du, Measuring out-of-time-order correlators on a nuclear magnetic resonance quantum simulator, *Physical Review X* **7**, 031011 (2017).
 - [17] N. Mirkin and D. Wisniacki, Quantum chaos, equilibration,

- and control in extremely short spin chains, *Physical Review E* **103**, L020201 (2021).
- [18] N. Chavda, H. Deota, and V. Kota, Poisson to goe transition in the distribution of the ratio of consecutive level spacings, *Physics Letters A* **378**, 3012 (2014).
- [19] B. N. Parlett, *The symmetric eigenvalue problem* (SIAM, 1998).
- [20] V. Viswanath and G. Müller, *The recursion method: application to many-body dynamics*, Vol. 23 (Springer Science & Business Media, 2008).
- [21] H. D. Simon, The lanczos algorithm with partial reorthogonalization, *Mathematics of computation* **42**, 115 (1984).
- [22] L. Fleishman and D. Licciardello, Fluctuations and localization in one dimension, *Journal of Physics C: Solid State Physics* **10**, L125 (1977).
- [23] Y. Atas, E. Bogomolny, O. Giraud, and G. Roux, Distribution of the ratio of consecutive level spacings in random matrix ensembles, *Physical review letters* **110**, 084101 (2013).
- [24] G. Lenz and F. Haake, Transitions between universality classes of random matrices, *Phys. Rev. Lett.* **65**, 2325 (1990).
- [25] G. Lenz, K. Życzkowski, and D. Saher, Scaling laws of the additive random-matrix model, *Phys. Rev. A* **44**, 8043 (1991).
- [26] P. Jacquod and C. Petitjean, Decoherence, entanglement and irreversibility in quantum dynamical systems with few degrees of freedom, *Adv. Phys.* **58**, 67 (2009).
- [27] A. Goussev, R. A. Jalabert, H. M. Pastawski, and D. A. Wisniacki, Loschmidt echo, *Scholarpedia* **7**, 11687 (2012).
- [28] I. García-Mata, R. A. Jalabert, and D. A. Wisniacki, Out-of-time-order correlations and quantum chaos, *Scholarpedia* **18**, 55237 (2023).